

Pair-correlation properties and momentum distribution of finite number of interacting trapped bosons in three dimension

Anindya Biswas^{1,a)}, Barnali Chakrabarti^{2,3} and Tapan Kumar Das¹¹

¹*Department of Physics, University of Calcutta, 92 A.P.C. Road, Kolkata 700009, India*

²*The Abdus Salam International Centre for Theoretical Physics, 34100, Trieste, Italy*

³*Department of Physics, Lady Brabourne College, P-1/2 Suhrawardy Avenue, Kolkata 700017, India*

We study the ground state pair-correlation properties of a weakly interacting trapped Bose gas in three dimension by using a correlated many-body method. Use of the van der Waals interaction potential and an external trapping potential shows realistic features. We also test the validity of shape-independent approximation in the calculation of correlation properties.

PACS numbers: 03.75.Hh, 03.65.Ge, 03.75.Nt

^{a)} Corresponding author e-mail : abc.anindya@gmail.com

I. INTRODUCTION

The last two decades have been witness to intense activities in experimental and theoretical study of correlation properties of interacting quantum systems. The problem is still challenging and open in the quantum many-body systems which are non-integrable. The task becomes simplified for integrable systems like one dimensional uniform Bose gas described by the Lieb-Liniger (LL) model [1,2], which assumes that particles interact via a δ -function repulsive potential. Since the experimental observation of Bose Einstein condensate (BEC) in ultracold trapped alkali atomic vapors, a lot of theoretical and experimental work has been done to study its correlation properties [3-12]. In the recent experimental situation, it is easy to achieve a quasi-one-dimensional strongly interacting degenerate Bose gas in a highly anisotropic trap [13-15] which is correctly described by the Lieb-Liniger model [16]. The complementary case is the weakly interacting (via finite range forces) trapped Bose gas. Although it is commonly believed that the Gross Pitaveskii (GP) equation is adequate for weakly interacting Bose gases, but a more rigorous and accurate many-body treatment, incorporating realistic interatomic interactions and interatomic correlations, is crucial for studying correlation properties in realistic condensates. The first motivation of the present work is to investigate the importance of finite size and trapping effects on the ground state correlation properties of ultracold atomic BECs. The second motivation of our study is to assess the validity of shape-independent approximation in the correlation properties. Dilute BECs are known to possess shape-independent (SI) property which is frequently described by the δ -function potential, whose strength is proportional to the s -wave scattering length (a_s). In the mean-field description, the effective interaction is determined by the factor Na_s (where a_s is expressed in units of oscillator length of the trap), whereas in the full many-body description we solve the many-body Schrödinger equation for different two-body potentials that generate identical a_s . Thus, our present calculation serves as a stringent test of the SI approximation and verifies whether the long range correlation at all affects the correlation properties or not. Inclusion of all possible two-body correlations in our *ab initio* many-body method correctly calculates correlation effects at zero temperature. Use of the realistic van der Waals interatomic potential with a long attractive tail provides the realistic aspects of the correlation function and its momentum distribution. Specially the effect of short range repulsion in the interatomic potential is expected to be reflected in the

pair correlation function.

The paper is organized as follows. In the next section, we briefly review our theoretical approach. In Section III, we present the results of our calculation of one-body density, pair distribution function and their momentum distributions. Finally, in Section IV we draw our conclusions.

II. POTENTIAL HARMONIC EXPANSION METHOD

We adopt the potential harmonics expansion method together with a short range correlation function (CPHEM), which has already been established as a successful and useful technique for investigating BEC with realistic two-body interactions. In the following, we briefly describe the technique. Interested readers can find the details in Refs.^{17–19}.

We start with the many-body Schrödinger equation of A spinless bosons trapped in an isotropic harmonic oscillator potential of frequency ω at zero temperature. The center of mass motion can be separated by introducing the center of mass vector (\vec{R}) and $N = A - 1$ Jacobi vectors $\{\zeta_1, \dots, \zeta_N\}$ defined as²⁰

$$\vec{\zeta}_i = \sqrt{\frac{2i}{i+1}} \left(\vec{x}_{i+1} - \frac{1}{i} \sum_{j=1}^i \vec{x}_j \right), \quad (i = 1, \dots, N), \quad (1)$$

where \vec{x}_i is the position vector of the i -th particle. The relative motion of the system is described by

$$\left[-\frac{\hbar^2}{m} \sum_{i=1}^N \nabla_{\zeta_i}^2 + V_{trap}(\vec{\zeta}_1, \dots, \vec{\zeta}_N) + V_{int}(\vec{\zeta}_1, \dots, \vec{\zeta}_N) - E_R \right] \psi(\vec{\zeta}_1, \dots, \vec{\zeta}_N) = 0, \quad (2)$$

where V_{trap} and V_{int} are respectively the trapping and pair-wise interaction potentials, expressed in terms of the Jacobi vectors. The energy of the relative motion is E_R . Next hyperspherical variables are introduced by defining a ‘hyperradius’

$$r = \left[\sum_{i=1}^N \zeta_i^2 \right]^{\frac{1}{2}}, \quad (3)$$

and a set of $(3N - 1)$ ‘hyperangles’, consisting of $2N$ polar angles of N Jacobi vectors and $(N - 1)$ angles defining their *relative lengths*²⁰. In the hyperspherical harmonics expansion method (HHEM) the N -body Schrödinger Equation (2) is solved by expanding ψ in the complete set of hyperspherical harmonics (HH), which are the eigenfunctions of the N -dimensional Laplace operator (analogous to the spherical harmonics in three dimension)²⁰. Substitution of this in Eq. (2) and projection on a particular HH results in a set of coupled differential equations. However imposition of symmetry of the wave function and calculation of the matrix elements are such formidable tasks that a practical solution for $A > 3$ is nearly impossible. Moreover due to the fact that the degeneracy of the HH basis increases very rapidly with the increase in the grand orbital quantum number K ²⁰, a convergent calculation using HHEM with *the full* HH basis is extremely computer intensive. This is the price one pays for keeping *all many-body correlations*. On the other hand, a typical experimental BEC is designed to be extremely dilute to eliminate the possibility of molecule formation through three-body collisions. Hence we assume that the probability of three and more particles to come within the range of interatomic interaction is negligible and the effect of the two-body correlations will be adequate for the full many-body wave function. Moreover, only two-body interactions are relevant. Therefore, ψ can be expressed in terms of Faddeev components ψ_{ij} of the (ij) interacting pair²¹

$$\psi = \sum_{i < j} \psi_{ij}(\vec{r}_{ij}, r). \quad (4)$$

Since only two-body correlations are important, ψ_{ij} is a function of the interacting-pair separation $r_{ij} = \vec{x}_i - \vec{x}_j$ and r only. Hence it can be expanded in the subset of HH needed for the expansion of the two-body interaction $V(\vec{r}_{ij})$. This subset is called the potential harmonics (PH) basis²¹. This results in a dramatic simplification in the analytic and computation works and it has been used upto 14000 bosons in the trap¹⁸. In this procedure, a realistic interatomic interaction can be used. Such an interaction has a strongly repulsive core. Hence ψ_{ij} must be vanishingly small for small values of r_{ij} . But the first ($K = 0$) term of the PH basis is a constant²⁰. Hence to reproduce the short-range behaviour of ψ_{ij} correctly, a large number of PH basis functions is needed, which slows down the rate of convergence considerably. Hence, we introduce a ‘short-range correlation function’ in the PH expansion basis²². In the zero temperature BEC, the kinetic energy of the interacting pair is practically zero. Therefore, the two-body collision process is determined entirely by

the s -wave scattering length (a_s). The small r_{ij} behavior of ψ_{ij} will be that of the zero-energy wave function $\eta(r_{ij})$ of the pair interacting via $V(r_{ij})$. Hence we introduce $\eta(r_{ij})$ as a short-range correlation function in the PH expansion¹⁹. We have checked explicitly that this improves the rate of convergence dramatically. In order that the small r_{ij} behavior of $\psi_{ij}(r_{ij}, r)$ corresponds to the correct two-body interaction appropriate for the experimental a_s , we adjust the very short-range behavior of the interatomic interaction (in the case of the van der Waals potential used by us, it will be the hard-core radius r_c) so that $\eta(r_{ij})$ asymptotically becomes proportional to $(1 - \frac{a_s}{r_{ij}})^{23}$. Substitution of this expansion of ψ in Eq. (2) and projection on a particular PH gives rise to a set of coupled differential equations in r ¹⁹

$$\begin{aligned} & \left[-\frac{\hbar^2}{m} \frac{d^2}{dr^2} + \frac{\hbar^2}{mr^2} \{ \mathcal{L}(\mathcal{L} + 1) + 4K(K + \alpha + \beta + 1) \} \right. \\ & \left. + V_{trap}(r) - E_R \right] U_{Kl}(r) \\ & + \sum_{K'} f_{Kl} V_{KK'}(r) f_{K'l} U_{K'l}(r) = 0, \end{aligned} \quad (5)$$

where $\mathcal{L} = l + (3A - 6)/2$, $U_{Kl}(r) = f_{Kl} u_K^l(r)$, $\alpha = \frac{3A-8}{2}$ and $\beta = l + \frac{1}{2}$. Here, l is the orbital angular momentum of the system (assumed to be contributed by the interacting pair only) and $u_K^l(r)$ is the coefficient of expansion of $\psi_{ij}(r_{ij}, r)$ in the correlated PH basis, while f_{Kl} represents the overlap of the PH corresponding to the (ij) -partition with the sum of PHs of all partitions¹⁸. Expressions for the potential matrix element $V_{KK'}(r)$ and f_{Kl} can be found in Ref.^{18,19}.

Eq. (5) is solved by hyperspherical adiabatic approximation (HAA)²⁴, for which we assume that the hyperangular motion is much faster than the hyperradial motion. Consequently, the former can be separated adiabatically and solved to obtain an effective potential as a parametric function of r , in which the hyperradial motion takes place. The hyperangular motion is effectively solved by diagonalizing the potential matrix $V_{KK'}(r)$ together with the hyper-centrifugal potential of Eq. (5) to get the lowest eigenvalue $\omega_0(r)$ [corresponding eigen column vector being $\chi_{K0}(r)$], which is the effective potential for the hyperradial motion. Finally, the adiabatically separated hyperradial equation

$$\left[-\frac{\hbar^2}{m} \frac{d^2}{dr^2} + \omega_0(r) + \sum_K \left| \frac{\chi_{K0}(r)}{dr} \right|^2 - E_R \right] \zeta_0(r) = 0. \quad (6)$$

is solved subject to appropriate boundary conditions to get E_R and the hyperradial wave function $\zeta_0(r)$. The many-body wave function can be constructed in terms of $\zeta_0(r)$ and $\chi_{K0}(r)$ ²⁴.

III. RESULTS

Now in order to study the correlation properties of the interacting Bose gas we choose a realistic interatomic potential having a strong repulsive core at a small separation and an attractive tail at large atomic separations. This is approximately represented by the van der Waals potential with a hard core of radius r_c and a $\frac{1}{r^6}$ attractive tail, *viz.* $V(r_{ij}) = \infty$, for $r_{ij} \leq r_c$ and $-\frac{C_6}{r_{ij}^6}$ for $r_{ij} > r_c$. The effective interaction is characterized by the s -wave scattering length (a_s), which depends strongly on r_c ²³. Usually the potentials are chosen to be purely attractive or purely repulsive according to whether a_s is negative or positive respectively. In our many-body calculation, we solve the zero-energy two-body Schrödinger equation with $V(r_{ij})$ to obtain a_s ^{19,23}. The value of r_c is adjusted so that a_s has the values corresponding to the JILA experiments^{25,26}. A typical value of r_c is of the order of 10^{-3} o.u. In atomic units this is a few tens of Bohr, which is larger than the atomic radius. Note that r_c is expected to be larger than the atomic radius, as the van der Waals potential with the hard core of radius r_c is the *effective potential* which produces the correct experimental *zero-energy* scattering cross-section (given by a_s).

A. One-body density

We define the one-body density, as the probability density of finding a particle at a distance \vec{r}_k from the center of mass of the condensate

$$R_1(\vec{r}_k) = \int_{\tau'} |\psi|^2 d\tau' \quad (7)$$

where ψ is the full many-body wave function and the integral over the hypervolume τ' excludes the variable \vec{r}_k . After a lengthy but straightforward calculation we arrive at a closed form given by

$$\begin{aligned}
R_1(\vec{r}_k) = & \sqrt{2} \int_0^\infty \int_{-1}^1 2^\alpha \left[\frac{1}{\pi^{3/2}} \frac{\Gamma((D-3)/2)}{\Gamma((D-6)/2)} \right] [\zeta_0(r')]^2 \\
& \sum_{KK'} \chi_{K0}(r') \chi_{K'0}(r') (f_{Kl} f_{K'l})^{-1} (h_K^{\alpha\beta} h_{K'}^{\alpha\beta})^{-1/2} P_K^{\alpha\beta}(z) \\
& P_{K'}^{\alpha\beta}(z) r'^{D-4} \sqrt{\frac{1+z}{2}} \left(\sqrt{\frac{1-z}{2}} \right)^{D-8} \\
& \left(\sqrt{r'^2 + 2r_k^2} \right)^{-(D-1)} dr' dz, \tag{8}
\end{aligned}$$

where $D = 3A - 3$ and $h_K^{\alpha\beta}$ is the norm of the Jacobi polynomial $P_K^{\alpha\beta}(z)$.

The one-body density contains information regarding one particle aspect of the bosonic system. Although it is not directly measurable but in the interferometry experiment one can indirectly explore it^{6,7}. In Fig.1 we present calculated one-body density as a function of the distance from the trap centre for a repulsive interaction corresponding to $a_s = .00433$ o.u. for 10000 ⁸⁷Rb atoms in the JILA trap²⁵. In our calculation, length and energy are measured in oscillator units (o.u.) of length $\left(a_{ho} = \sqrt{\frac{\hbar}{m\omega}} \right)$ and energy $(\hbar\omega)$ respectively. For comparison, we also include the mean-field results. The effect of interaction is revealed by the deviation from the Gaussian profile. To explore the effect of interaction, we also calculate one-body density for a smaller a_s value *viz.*, $a_s = 2.09 \times 10^{-4}$ o.u. for the same number of particles. Since the trapped condensate is always stable even for a large A , we see appreciable changes in $R_1(\vec{r}_k)$ as a_s decreases. For small a_s , the density distribution is sharper as the correlations induced by the interactions are weak, while for the larger a_s , the peak is flatter with a larger width. In Fig. 2 we present calculated one-body density for an attractive BEC with $a_s = -1.836 \times 10^{-4}$ o.u for different number of ⁸⁵Rb atoms in the JILA trap²⁶. The effective interaction parameter is $\lambda = A|a_s|/a_{ho}$. For $A= 100$, λ is small and the system exhibits weak one-body density which extends to the trap size. Increasing A gradually, the net effective attraction becomes strong and the density becomes sharply peaked at a smaller distance.

Taking the Fourier transform of $R_1(\vec{r}_k)$, we obtain the one-body momentum distribution. One-body density is an abstract concept. However, its fourier transform gives the experimentally measurable quantity, the momentum distribution. In Fig. 3, we plot our results for repulsive interactions. It evolves from a Gaussian in the noninteracting limit to a curve

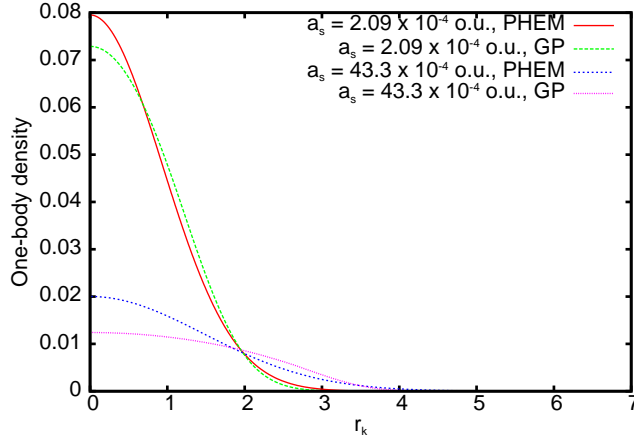


FIG. 1. (Color online) One-body density distribution as a function of r_k (in o.u.) for a repulsive BEC with $A=10000$ bosons. The choice of $a_s = 0.00433$ o.u. corresponds to ^{87}Rb experiment in the JILA trap. PHEM corresponds to our present many-body results and GP corresponds to mean-field results.

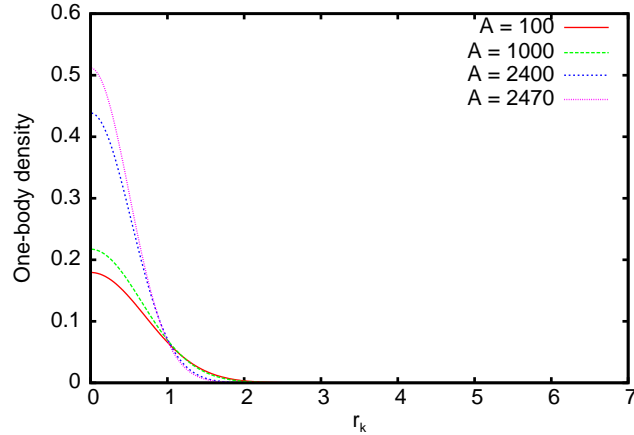


FIG. 2. (Color online) One-body density distribution as a function of r_k (in o.u.) for an attractive interaction ($a_s = -1.836 \times 10^{-4}$ o.u. for ^{85}Rb atoms in the JILA trap), for various indicated values of particle numbers.

having a sharper peak, as the net interaction increases. The peak at $k = 0$ becomes more pronounced with increase in effective repulsion, whereas for weak interaction it develops a long-range tail in the momentum space. The momentum is being redistributed to higher k values. The width of the low-momentum peak for $a_s = 0.00433$ o.u. and $A = 10000$ is about $0.7 \mu\text{m}^{-1}$.

We have remarked earlier that with recent progress in creating atomic clouds with large dipole moment, interest has been shifted to longer range interaction instead of taking only

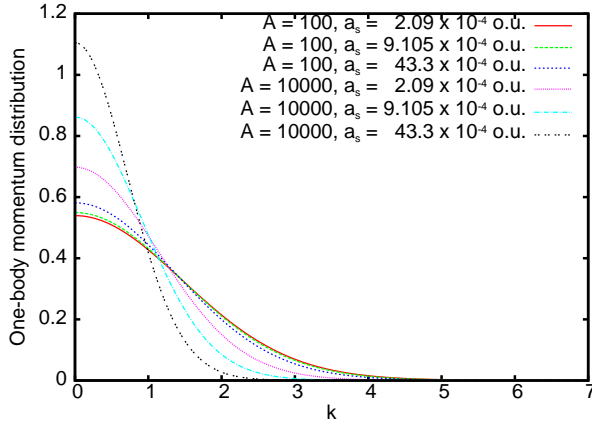


FIG. 3. (Color online) Calculated one-body momentum distribution for the repulsive BEC for different values of A and a_s . The choice of $a_s = 0.00433$ o.u. corresponds to ^{87}Rb experiment in JILA trap. All quantities are in appropriate oscillator units.

contact interaction. Thus, even in the low-density limit the use of a realistic interatomic interaction potential in the many-body calculation has been emphasized by several authors [27–29]. The van der Waals potential is an ideal choice as it properly takes care of the effect of realistic dipole-dipole interaction. The strength of the van der Waals interaction C_6 changes widely from a small value for H atoms to a high value for Cs atoms. Hence, to see how the one-body density is affected by the strength of the long-range tail of the two-body potential, we select three different values of C_6 in addition to the actual experimental value – one below and two above. These are (in o.u.): 5×10^{-11} , 6.489755×10^{-11} , 8.5×10^{-11} , 8×10^{-10} , the second one being the experimental value. For each value of C_6 , we calculate corresponding r_c as before, such that a_s has the experimental value 0.00433 o.u. For each set of (C_6, r_c) , we solve the many-body Schrödinger equation as before. Calculated one-body density for different sets are shown in Fig. 4 for 10000 bosons. We observe that the one-body density of the inhomogeneous gas for different two-body potentials are almost indistinguishable; i.e. independent of the shape of $V(r_{ij})$. Our numerical calculations confirm that one-body density is absolutely determined (within numerical errors) by the parameter a_s only.

This is in contrast with ref.²⁹, where ground state energy of the condensate was found to depend on the shape of the potential. Thus the one-body density does not depend strongly on the shape of the interaction potential, while the ground state energy does.

An explanation of the above observation is as follows. The total condensate energy

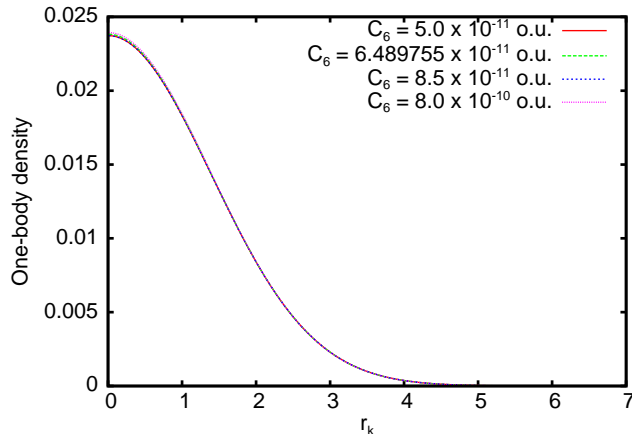


FIG. 4. (Color online) One-body density distribution for the repulsive BEC with several C_6 parameters, all of which correspond to the identical $a_s = 0.00433$ o.u., with 10000 ^{87}Rb atoms in the JILA trap. All quantities are in oscillator units.

depends on the minimum of the well, in addition to the actual shape of the lowest eigen potential. In Table 1, we present the dependence of the position (r_m) and the value (ω_{0m}) of the minimum of lowest eigen potential for different values of C_6 parameter, corresponding to the same a_s .

Table 1. Dependence of r_m and ω_{0m} on C_6 (corresponding to $a_s = 0.00433$) for $A = 10000$ atoms (all quantities are expressed in o.u.).

C_6	r_m	ω_{0m}
5.0×10^{-11}	339.92	48792.7
6.4×10^{-11}	339.47	48668.7
8.5×10^{-11}	339.04	48546.3
8.0×10^{-10}	338.93	48517.8

We observe that, as C_6 increases, ω_{0m} decreases appreciably, while position of the minimum of effective many-body potential changes by a small amount. In the next sub-section, we will see that the shape of the $\omega_0(r)$ curve remains practically unchanged. As the total condensate energy depends on the depth of the potential, as well as on its shape (stiffness), we observe that the ground state energy decreases gradually with increase in C_6 ²⁹. Thus the shape independence hypothesis is violated for the total energy. However, the one-body density distribution is given by the many-body wave function, which is independent of the

minimum of the potential, but depends only on its shape. Hence it remains unchanged with change in C_6 parameter and shape independence of the one-body density profile is satisfied.

B. Pair distribution function

Another key quantity is the pair distribution function $R_2(r_{ij})$, which determines the probability of finding the (ij) -pair of particles at a relative separation r_{ij} . The study of pair correlation is important, since the interatomic interactions play a crucial role as there are two competing interaction length scales. When the atoms try to form clusters, a strong very short range repulsion in atomic interaction comes into play. As atoms repel each other strongly at very small separations it is impossible to get some non-vanishing value of $R_2(r_{ij})$ at $r_{ij} = 0$. We calculate it as

$$R_2(r_{ij}) = \int_{\tau''} |\psi|^2 d\tau'', \quad (9)$$

where ψ is the many-body wavefunction and the integral over the hypervolume τ'' excludes integration over r_{ij} . Again after a lengthy calculation we can put it in a closed form given by

$$R_2(r_{ij}) = \sqrt{2} \int_{-1}^1 \left(\frac{1-z}{2}\right)^\alpha \left(\zeta_0 \left(r_{ij} \sqrt{\frac{2}{1+z}}\right)\right)^2 \sum_{KK'} \left(\frac{h_K^{\alpha\beta}}{2^\alpha}\right)^{-1/2} \left(\frac{h_{K'}^{\alpha\beta}}{2^\alpha}\right)^{-1/2} (f_{Kl} f_{K'l})^{-1} \chi_{K0}(r) \chi_{K'0}(r) P_K^{\alpha\beta}(z) P_{K'}^{\alpha\beta}(z) dz. \quad (10)$$

We plot $R_2(r_{ij})$ in Fig. 5 for the attractive interaction with different particle numbers. As mentioned earlier, pair correlation vanishes as $r_{ij} \rightarrow 0$, due to the strong interatomic repulsion and it cannot extend beyond the size of the condensate. Hence R_2 is peaked at some intermediate value of r_{ij} . For weak interactions (small λ), the correlation length is large. However as the effective attractive interaction increases, two interacting particles come closer and the pair-correlation length decreases; the pair distribution function becomes sharply peaked. It indicates stronger pair correlation in the system, in agreement with expectations. However our results are at variance with those obtained in LL model⁸, which describes uniform systems with no confinement. Consequently pair correlation function

approaches its maximum asymptotically, whereas in our confined three dimensional case, it vanishes asymptotically. When A is increased to 2470, which is very close to the critical number ($A_{cr} \simeq 2475$), the effect is quite prominent. As the width of the curves decrease with increase in effective attractive interaction, the interacting pair becomes more localized. This manifests the possibility of clustering due to large two-body interaction and three-body recombination, if the attraction becomes strong enough. This will lead to an eventual collapse of the attractive condensate, when the pair-correlation length will drastically reduce to a very small value and the condensate will be destroyed.

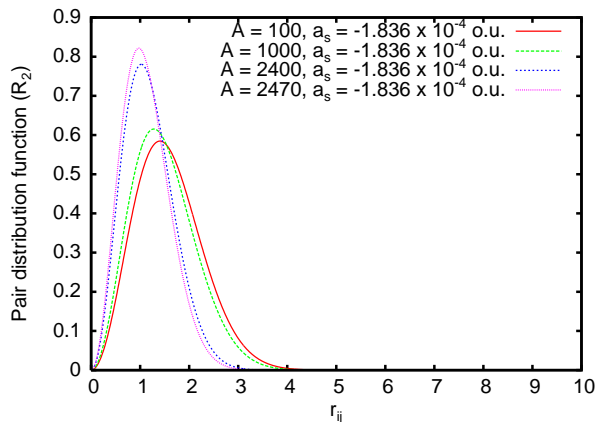


FIG. 5. (Color online) Plot of pair distribution function ($R_2(r_{ij})$) against r_{ij} (in o.u.) for an attractive Bose gas with different particle numbers in the trap.

Two-particle correlation is directly related with pair inelastic processes and can be directly measured in photoassociation in interatomic collisions. As the attractive interaction increases, the gas becomes highly correlated and different inelastic processes may take place. The opposite case is the repulsive Bose gas where the pair inelastic process will be suppressed with increase in interaction. For completeness, in Fig. 6 we plot the relative momentum distribution obtained as the Fourier transform of $R_2(r_{ij})$ for various particle numbers for ^{87}Rb condensate in the JILA trap, with $a_s = 0.00433$ o.u. (100 a.u.). The width of the curve decreases and exhibits a sharp peak at $k = 0$, whose height increases with increasing number of particles.

Lastly to visualize the effect of different strength parameter C_6 on the pair-correlation, we plot $R_2(r_{ij})$ against r_{ij} for the previous sets of potential parameters in Fig. 7. We find

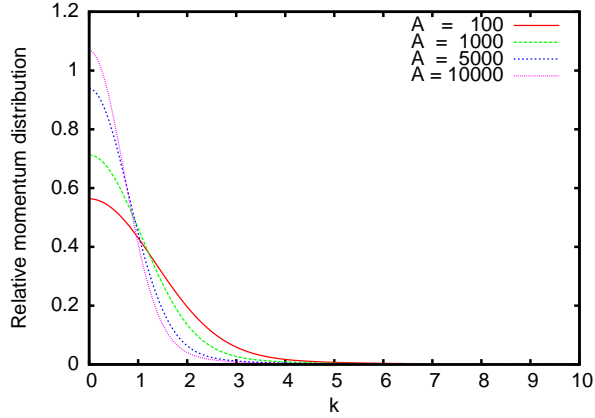


FIG. 6. (Color online) Plot of relative momentum distribution against k (in $(\text{o.u.})^{-1}$) for various indicated values of particle numbers. The choice of $a_s = 0.00433$ o.u. corresponds to ^{87}Rb experiment in JILA trap.

that different interatomic potential shapes corresponding to the same a_s produce identical correlation properties, which indicates that the calculated property is independent of the shape of the two-body potential. The fact that the ground state energy is dependent on the shape of the two-body potential²⁹ whereas the one-body density and the pair distribution function are not, can be attributed to the fact that the many-body wave function remains invariant irrespective of the variation of the shape of the two-body potential due to variation of (C_6, r_c) for the same value of a_s . Note that the condensate wave function in the hyperradial space $\zeta_0(r)$ is obtained by solving the hyperradial equation (6) in the effective many-body potential $\omega_0(r)$. The shape and stiffness of this effective potential remain unchanged for the same value of a_s , irrespective of the variation of the shape of the two-body potential. However, as discussed earlier, the position and value of the minimum of the effective many-body potential change with the variation of the parameter C_6 . To demonstrate this, we plot the effective many-body potential $\omega_0(r)$ as a function of r for various values of C_6 in Fig. 8. The curves have been shifted both vertically and horizontally in order that the minima coincide (both in position and value). One observes that all the curves overlap completely (within numerical errors) showing that the shape and stiffness of the effective potential remain invariant. Hence the kinetic energy and the wave function remain unchanged, while potential energy and the total energy change with change of C_6 . By direct numerical calculation, we have checked that the change of kinetic energy is very small compared with that of the total energy, as C_6 varies. Therefore the ground state energy is shape dependent, whereas the

one-body density and pair distribution function are not.

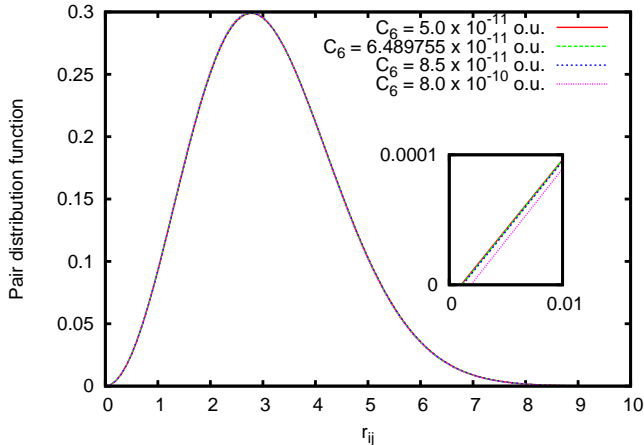


FIG. 7. (Color online) Plot of two-body correlation function against r_{ij} in o.u. for repulsive BEC with several indicated C_6 parameters, all of which correspond to identical $a_s = 0.00433$ o.u. with 10000 ^{87}Rb atoms in JILA trap. (The portion near the origin is magnified in the inset to show that the pair distribution function vanishes inside the hard core. The same is true for Fig. 5.)

IV. CONCLUSION

In conclusion, the present work focuses on the one-body density and pair-correlation aspects of the zero temperature weakly interacting trapped Bose gas. The use of correlated many-body approach takes care of the effect of finite-size, where quantum fluctuation is important and gives a realistic picture of correlation properties. Due to the use of a realistic interatomic interaction and consideration of finite number of atoms in the trap, our results deviate from the earlier results^{4,8}, but exhibit realistic aspects which are relevant to experiments. Our calculation is performed for a two-body potential (van der Waals potential), whose parameters can be adjusted to give both positive and negative scattering lengths, for Rb atoms in the JILA trap. Thus, our results are realistic and can be experimentally verified in future. Our calculations also verify the validity of the shape-independent approximation in dilute BECs for one-body density and pair-distribution functions. This is in contrast with the earlier observed shape dependence for ground state energies²⁹.

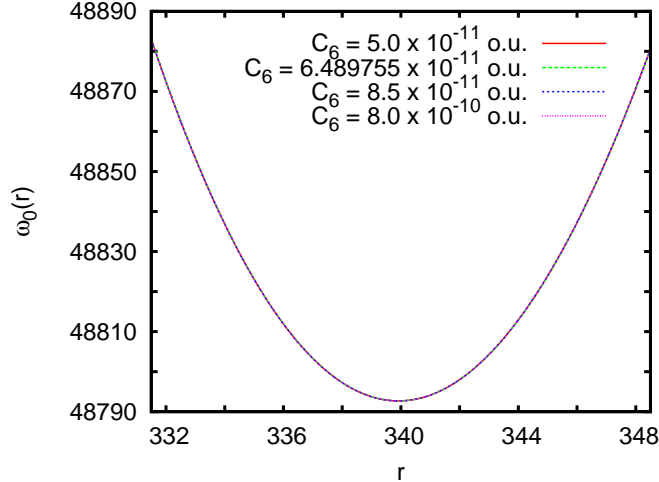


FIG. 8. (Color online) Plot of the effective potential (in o.u.) against r (in o.u.) for 10000 ^{87}Rb atoms with $a_s = 0.00433$ o.u.. The curve corresponding to $C_6 = 5.0 \times 10^{-11}$ is in its actual position. The other curves have been shifted both vertically and horizontally to coincide the minima (both in position and value). All the curves overlap completely (within numerical errors). This shows that the shape of the effective many-body potential $\omega_0(r)$ is independent of the choice of (C_6, r_c) for the same value of a_s .

Acknowledgement

We would like to acknowledge helpful discussion with L. Salasnich, S.R. Jain and G. Mus-sardo. This work has been funded by the Department of Science and Technology (DST), India under grant number SR/S2/CMP/0059(2007). BC thanks the International Center for Theoretical Physics (ICTP), Trieste for hospitality and financial support, where a part of the work was done. TKD acknowledges the University Grants Commission (UGC), India for the Emeritus Fellowship. AB acknowledges the UGC, India for the Research Fellowship in Sciences for Meritorious Students and the Council of Scientific and Industrial Research (CSIR), India for a Senior Research Fellowship.

REFERENCES

- ¹E. H. Lieb and W. Liniger, Phys. Rev. **130**, 1605 (1963).
- ²E. H. Lieb, Phys. Rev. **130**, 1616 (1963).
- ³K. Sakman *et al*, Phys. Rev. A **78**, 023615 (2008).

- ⁴M. Naraschewski and R.J.Glauber, Phys. Rev. A **59**, 4595 (1999).
- ⁵L. E. Sadler *et al*, Phys. Rev. Lett. **98**, 110401 (2007).
- ⁶S. Ritter *et al*, Phys. Rev. Lett. **98**, 090402 (2007).
- ⁷I. Bloch, T.W. Hänsch and T.Esslinger, Nature(London), **403**, 166 (2000).
- ⁸G. E. Astrakharchik and S. Giorgini, Phys. Rev. A **68**, 031602(R) (2003).
- ⁹S.Zöllner, H.D.Meyer and P.Schmelcher, Phys. Rev. Lett. **100**, 040401 (2008).
- ¹⁰R. Pezer and H. Buljan, Phys. Rev. Lett. **98**, 240403 (2007).
- ¹¹K. V. Kheruntsyan *et al*, Phys. Rev. Lett. **91**, 040403 (2003).
- ¹²D. M. Gangardt and G. V. Shlyapnikov, Phys. Rev. Lett. **90**, 010401 (2003).
- ¹³M. Greiner *et al*, Phys. Rev. Lett. **87**, 160405 (2001).
- ¹⁴F. Schreck *et al*, Phys. Rev. Lett. **87**, 080403 (2001).
- ¹⁵A. Görlitz *et al*, Phys. Rev. Lett. **87**, 130402 (2001).
- ¹⁶D. M. Gangardt and G.V. Shlyapnikov, New Journal of Phys. **5**, 79 (2003).
- ¹⁷T.K.Das and B.Chakrabarti, Phys. Rev. A **70**, 063601, (2004).
- ¹⁸T.K.Das, S. Canuto, A. Kundu and B. Chakrabarti, Phys. Rev. A **75**, 042705, (2007).
- ¹⁹T. K.Das, A. Kundu, S. Canuto and B. Chakrabarti, Phys. Letts. A **373**, 258 (2009).
- ²⁰J.L.Ballot and M.Fabre de la Ripelle, Ann. Phys. (N.Y.) **127**, 62, (1980).
- ²¹M.Fabre de la Ripelle, Ann. Phys. (N.Y.) **147**, 281, (1983).
- ²²C. D. Lin Phys. Rep. **257**, 1 (1995).
- ²³C.J. Pethick and H. Smith, Bose-Einstein condensation in dilute gases, Cambridge University Press, Cambridge, (2001).
- ²⁴T.K.Das, H.T.Coelho and M.Fabre de la Ripelle, Phys. Rev. C **26**, 2281, (1982).
- ²⁵M. H. Anderson *et al*, Science **269**, 198 (1995).
- ²⁶J.L. Roberts *et al*,Phys. Rev. Lett. **86**, 4211, (2001).
- ²⁷B. Gao, J. Phys. B **36**, 2111 (2003).
- ²⁸S. Geltman, J. Phys. B **37**, 315 (2004).
- ²⁹B. Chakrabarti and T. K. Das, Phys. Rev. A **78**, 063608 (2008).